NUCLEAR MAGNETIC RELAXATION IN A SPIN 1 SYSTEM

K.R. Jeffrey

Department of Physics
University of Guelph
Guelph, Ontario, Canada

I. INTRODUCTION

Deuterium nuclear magnetic resonance (^{2}HNMR) has become a very valuable tool in the study of the structure and dynamics of anisotropic fluids, especially lipid bilayer model and biological membranes (1,2). Because the deuterium nucleus has spin $I = 1$, there is a quadrupolar splitting of the nuclear Zeeman resonance line into a doublet whenever the nucleus experiences a non-zero electric field gradient. In anisotropic fluids, the quadrupolar splitting for deuterons, which have been substituted for hydrogen atoms bonded to carbon atoms, gives a direct measure of the orientational order parameter for the C - D bond. This parameter can be related to fundamental structural and dynamical properties of these systems (1). While ^{2}HNMR spectroscopy is a well established technique, the use of the nuclear magnetic relaxation times to study the dynamics of anisotropic fluids is just beginning (3,4).

For a system of noninteracting spins, $I = ½$, there are two relaxation times, commonly called the spin-spin and spin-lattice relaxation times T_2 and T_1, respectively.

For the case of spin $I = 1$ nuclei, where there is a non-vanishing electric quadrupole interaction, there are 5 independent relaxation times to be measured (5). One of these is associated with the return of the Zeeman energy to its equilibrium value and is therefore called T_{1Z}, another is associated with the decay of the quadrupolar energy, T_{1Q}, and there are three independent spin-spin relaxation times. Jacobsen and Schaumberg (6), using adiabatic rapid passage techniques, measured T_{1Z} and T_{1Q} separately for the deuterium quadrupolar doublet of D_2O in an oriented lyotropic liquid crystal system. Vold and Vold (7) reanalysed the relaxation behaviour for a spin 1 system using the Redfield formalism (8) and showed how T_{1Z}, T_{1Q}, and one spin-spin relaxation time, T_2, could be measured using selective and non-selective pulse techniques. T_2 is the relaxation time which can be obtained from a measurement of the linewidth in the absence of temperature, field, and other macroscopic inhomogeneities. T_2 also describes the decay of the quadrupolar echo (9) as a function of the spacing between the two radio frequency (RF) pulses used to form the echo. The techniques of Vold and Vold are applicable to the very narrow line spectra found in thermotropic liquid

crystals. However, the linewidths in lyotropic liquid crystals, especially model membranes, preclude the use of selective pulses. In many circumstances, unoriented or powder samples must be used.

Ahmad and Packer (10,11), using the Redfield formalism, have considered the response of a spin 1 system to two three-pulse sequences when there are both secular and time dependent quadrupolar interactions. The two sequences are denoted by

$$(\pi/2)_x - \tau - (\pi/4)_y - T - (\pi/4)_y$$

and

$$(\pi/2)_x - \tau - (\pi/2)_y - T - (\pi/2)_y$$

where the symbol $(\theta)_k$ indicates an RF pulse applied along the k axis for a time $\theta = \gamma H_1 t$. H_1 is the strength of the RF magnetic field. The $(\pi/2)_x - \tau - (\pi/4)_y - T - (\pi/4)_y$ sequence, commonly called the Jeener-Broekaert sequence (12), is of particular importance because it provides a means of measuring T_{1Q}. This sequence and the conventional $(\pi)_x$ - τ - $(\pi/2)_x$ sequence were used to measure T_{1Q} and T_{1Z} for the deuterium quadrupole doublet of D_2O in an oriented lyotropic liquid crystal system (11).

Vega and Pines (13) have developed an operator formalism in terms of nine fictitious spin ½ operators in order to present a very clear picture of the evolution of a spin 1 system in the presence and absence of RF fields. However, they did not consider the effects of relaxation.

In the present discussion, the operator formalism of Vega and Pines (13) is used to develop a number of pulse techniques suitable for measurement of the relaxation times for a spin 1 system. While some of these have already appeared in the literature, it is worthwhile presenting a complete picture using one formalism. In addition, the various techniques will be illustrated using two anisotropic fluid samples. The first is a mixture of 30% potassium laurate-αd_2, 60% H_2O, 6% decanol, and 4% potassium chloride. This sample is a nematic lyotropic liquid crystal (14). The spectrum of the deuterons in the α position in the potassium laurate molecule is a single doublet pattern characteristic of a spin 1 system in an oriented sample. There is a single angle equal to 90° between the effective axis of symmetry of the electric field gradient and the magnetic field. The other sample is a mixture of 70% rubidium stearate-αd_2 and 30% H_2O and is also a lyotropic liquid crystal but the stearate molecules do not orient in the magnetic field. The deuterium spectrum is a typical powder pattern, indicating that the angle between the axis of symmetry of the electric field gradient and the magnetic field may take all possible values.

II. MEASUREMENT OF RELAXATION TIMES IN A SPIN 1 SYSTEM

A Relaxation Times for a Spin 1 System

The Hamiltonian for a system of non-interacting spins, $I = 1$, in an external magnetic field with a non-vanishing electric quadrupole interaction can be written as

$$\mathcal{H} = \mathcal{H}_Z + \langle \mathcal{H}_Q(t) \rangle + \mathcal{H}_{RF} + [\mathcal{H}_Q(t) - \langle \mathcal{H}_Q(t) \rangle] \quad (1)$$

where

$$\mathcal{H}_Z = \hbar \omega_0 I_z \quad (2)$$

is the Zeeman interaction and

$$\langle \mathcal{H}_Q(t) \rangle = (\hbar \omega_Q / 3)\,[3I_z^2 - I(I+1)] \quad (3)$$

is the secular or static part of the electric quadrupole interaction. The Zeeman interaction strength in angular units is

$$\omega_0 = \gamma \mathcal{H}_0$$

while the quadrupolar interaction strength is

$$\omega_Q = \Delta_Q\,[(3\cos^2\theta - 1)/2 + \eta \sin^2\theta \cos 2\psi] \quad (4)$$

where

$$\Delta_Q = 3\{e^2 qQ/(2I-1)\}/2. \quad (5)$$

The orientation of the principal axes of the quadrupole interaction tensor with respect to the external magnetic field is given by the angles θ and ψ, and η is the asymmetry parameter. It will be assumed that $\omega_Q << \omega_0$ and that only the first order perturbation of the quadrupolar interaction on the Zeeman Hamiltonian need be considered. The Zeeman and static quadrupolar interactions determine the observed deuteron spectrum.

The interaction of the spin with RF radiation is described by

$$\mathcal{H}_{RF} = 2\hbar \omega_1 I_x \cos(\omega t + \phi) \quad (6)$$

where $2\hbar\omega_1$ is the RF irradiation strength at frequency ω. The relaxation of the spin system back to equilibrium is determined by the time dependent part of the quadrupolar interaction

$$\mathcal{H}_r(t) = \mathcal{H}_Q - \langle \mathcal{H}_Q(t) \rangle \cdot$$

The relaxation Hamiltonian may be written

$$\mathcal{H}_r(t) = eQ/[6I(2I-1)]$$
$$\sum_{\gamma\beta} V_{\gamma\beta}(t)[3/2(I_\gamma I_\beta + I_\beta I_\gamma) - \delta_{\gamma\beta} I^2] \quad (7)$$

where (γ,β = x,y,z) and the $V_{\gamma\beta}$ are the components of the electric field gradient tensor in the laboratory frame.

The dynamics of the spin system are best dealt with in terms of the density matrix. The time dependence of the density matrix is described by

$$d\varrho(t)/dt = i/\hbar\,[\mathcal{H}\varrho] \quad (8)$$

In order to eliminate the effect of the large Zeeman interaction, Eq. 8 is transformed into the rotating frame. Using the unitary operator

$$S = \exp(-i\omega t I_z) \quad (9)$$

the equation of motion becomes

$$d\varrho/dt = i/\hbar\,[\varrho,\ V + \mathcal{H}_r(t)] \quad (10)$$

where $\varrho = S\varrho S^{-1}$

$$V = \hbar\Delta\omega I_z + 1/3\,\hbar\omega_Q(3I_z^2 - I^2) + \hbar\omega_1 I_x,$$

and

$$\mathcal{H}_r(t) = S\mathcal{H}_r(t)S^{-1}.$$

Eq. 10 still has both time-dependent and time-independent parts of the Hamiltonian in the commutator. In order to remove the time-independent part, a further transformation to an interaction representation is performed. The transformation is defined by

$$T = \exp(-i\Delta\omega t I_z + 1/3\,i\omega_Q t(3I_z^2 - I^2) + i\omega_1 t). \quad (11)$$

The equation of motion in this representation is

$$d\varrho^*/dt = i/\hbar\,[\varrho^*, \mathcal{H}_r^*(t)] \quad (12)$$

where

$$\varrho^* = T\varrho T^{-1}$$

and

$$\mathcal{H}_r^*(t) = T\mathcal{H}_r T^{-1}$$

Provided that the relaxation is sufficiently weak, the effects of $\mathcal{H}_r(t)$ can be evaluated using time-dependent perturbation theory (14) which leads to the approximate equation

$$d\varrho^*/dt = -1/2\hbar^2 \int_{-\infty}^{\infty} [\mathcal{H}_r^*(t),$$
$$[\mathcal{H}_r^*(t-\tau), (\varrho^*(t) - \varrho^*_{eq})]\,d\tau \quad (13)$$

where the bar indicates an ensemble average and ϱ^*_{eq} is the equilibrium density matrix.

To obtain the equation of motion for ϱ, the density matrix in the rotating frame, it is necessary to transform back into that frame.

$$d\varrho/dt = i/\hbar\,[\varrho,\ V] -$$
$$1/2\hbar^2 \int_{\infty}^{\infty} [\mathcal{H}_r(t),\ e^{-iV\tau}\mathcal{H}_r(t-\tau)\,e^{iV\tau},\ (\varrho(t) - \varrho_{eq})]\,d\tau \quad (14)$$

If the molecular motion which gives rise to the time dependence of $\mathcal{H}_r$ is characterized by a correlation time τ_c, then Eq. 13 is valid if $[|\mathcal{H}_r(t)|^2\tau_c^{\,2}]^{1/2}$ is a small number.

Following the approach of Hoffman (15), the density matrix is expanded in terms of operators formed from the spin angular momentum operators. For a spin 1 system, the density matrix may be expanded in terms of the unit operator Q_1 and eight other independent operators $Q_2 \ldots Q_8$. Vega and Pines (13) have used nine symmetrized operators, of which eight are independent, and the unit operator. The nine operators I_{pi}, where p = x,y,z and i = 1,2,3, are given by

$$I_{p1} = 1/2\,I_p \quad (15)$$

$$I_{p2} = 1/2(I_q I_r + I_r I_q) \quad (16)$$

$$I_{p3} = 1/2(I_r^2 - I_q^2) \quad (17)$$

The symbols p,q,r are cyclic permutations of x,y,z. It should be noted that

$$I_{x3} + I_{y3} + I_{z3} = 0 \quad (18)$$

Wokaun and Ernst (16) have chosen to use a set of different linear combinations of these operators while Jacobsen *et al* (5) have chosen to use the irreducible tensor operators of first and second rank derived from the spin angular momentum operators.

For this discussion, it is convenient to define a set of operators Q_j (j = 1-9) where Q_1 is the unit operator, $Q_2 \ldots Q_7$ are the six operators defined by Eqs. 15 and 16, and

$$Q_8 = I_{z3} = 1/2(I_x^2 - I_y^2) \quad (19)$$

$$Q_9 = I_{x3} - I_{y3} = 1/2(3I_z^2 - I^2). \quad (20)$$

The density matrix may be expanded as

$$\varrho(t) = \sum_j A_j(t)\,Q_j \quad (21)$$

The time dependence is contained solely within the coefficients $A_j(t)$.

The observed signals in an NMR apparatus are proportional to $\mathrm{tr}(\varrho I_x)$ and $\mathrm{tr}(\varrho I_y)$ and are therefore pro-

portional to the coefficients A_2 and A_3. An NMR spectrometer having quadrature detection has two receiver channels (Labelled and X and Y channels) and is able to simultaneously observe the signals proportional to A_2 and A_3. The Zeeman energy is proportional to A_4 while the quadrupolar energy is proportional to A_9. The description of the double quantum coherence (13) of the system is contained in the coefficients A_7 and A_8. Substitution of Eq. 21 into Eq. 14 results in a set of equations for the coefficients $A_j(t)$

$$A_j(t) = i\sum_k \{\mathrm{tr}[Q_jQ_k]/\mathrm{tr}Q_j^2\}A_k(t) + 1/\{2\hbar^2\mathrm{tr}[Q_j^2]\} \int_{-\infty}^{\infty} \overline{[Q_j, \mathcal{H}_r(t)]\,[Q_j,\, e^{-iv\tau}\,\mathcal{H}(t-\tau)\,e^{-iv\tau}\,\mathcal{H}(t-\tau)\,e^{iv\tau}]}\,d\tau \{A_j(t) - A_j^{eq}\} \quad (22)$$

These equations describe the evolution of the density matrix during the application of an RF pulse and, if ω_1 is set equal to zero, the evolution in the intervals between pulses. The relaxation Hamiltonian, Eq. 7, can also be written in terms of the operators Q_j. The resulting equation is

$$\mathcal{H}_r = K\{V_{zz}Q_9 + (V_{yy} - V_{xx})\,Q_8 + 2V_{xy}Q_7 + 2V_{zx}Q_6 + 2V_{yz}Q_5\} \quad (23)$$

In the theory to follow, only pulses which satisfy the condition $\omega_1 >> \omega_Q$ will be considered, and it will be assumed that the duration of the pulses is short enough that relaxation during the pulse can be neglected. Under these circumstances, the effect of an RF pulse can be easily tabulated as has been done by Vega and Pines (Table V in reference 10). The sudden changes in the coefficients A_j that occur with the application of pulses along the x and y directions are given in Table 1.

Table 1
The Effect of a Strong Radio Frequency Pulse

(a) Applied in the X Direction

A_2	A_2
A_3	$A_3\cos\omega_1 t - A_4\sin\omega_1 t$
A_4	$A_4\cos\omega_1 t + A_3\sin\omega_1 t$
A_5	$A_5\cos 2\omega_1 t + (A_8/2)\sin 2\omega_1 t - (A_9/2)\sin 2\omega_1 t$
A_6	$A_6\cos\omega_1 t + A_7\sin\omega_1 t$
A_7	$A_7\cos\omega_1 t - A_6\sin\omega_1 t$
A_8	$(A_8/4)(3 + \cos 2\omega_1 t) + (A_9/4)(1 - \cos 2\omega_1 t) - (A_5/2)\sin 2\omega_1 t$
A_9	$(3A_8/4)(1 - \cos 2\omega_1 t) + (A_9/4)(1 + 3\cos 2\omega_1 t) + (3A_5/2)\sin 2\omega_1 t$

(b) Applied in the Y Direction

A_2	$A_2\cos\omega_1 t + A_4\sin\omega_1 t$
A_3	A_3
A_4	$A_4\cos\omega_1 t - A_2\sin\omega_1 t$
A_5	$A_5\cos\omega_1 t - A_7\sin\omega_1 t$
A_6	$A_6\cos 2\omega_1 t + (A_8/2)\sin 2\omega_1 t + (A_9/2)\sin 2\omega_1 t$
A_7	$A_7\cos\omega_1 t + A_5\sin\omega_1 t$
A_8	$(A_8/4)(3 + \cos 2\omega_1 t) - (A_9/4)(1 - \cos 2\omega_1 t) - (A_6/2)\sin 2\omega_1 t$
A_9	$-(3A_8/4)(1 - \cos 2\omega_1 t) + (A_9/4)(1 + 3\cos 2\omega_1 t) - (3A_6/2)\sin 2\omega_1 t$

After a pulse has been applied, the spin system evolves in the rotating frame under the influence of V and $\mathcal{H}_r(t)$. In the particular case where the spin system is exactly at resonance and no RF power is being applied, the equations of motion of the coefficients A_j derived from Eq. 20 are

$$dA_2/dt = -\omega_Q A_5 - A_2/T_{2a} \quad (24)$$

$$dA_3/dt = \omega_Q A_6 - A_3/T_{2a} \quad (25)$$

$$dA_4/dt = (A_4 - A_4^{eq})/T_{1Z} \quad (26)$$

$$dA_5/dt = \omega_Q A_2 - A_5/T_{2b} \quad (27)$$

$$dA_6/dt = -\omega_Q A_3 - A_6/T_{2b} \quad (28)$$

$$dA_7/dt = -A_7/T_{2D} \quad (29)$$

$$dA_8/dt = -A_8/T_{2D} \quad (30)$$

$$dA_9/dt = -A_9/T_{1Q} \quad (31)$$

The relaxation times introduced in Eq. 24 to 31 are defined as follows

$$1/T_{2a} = K[3J_0(0)/4 + 5J_1(\omega_0)/2 + J_2(2\omega_0)] \quad (32)$$

$$1/T_{2b} = K[3J_0(0)/4 + J_1(\omega_0)/2 + J_2(\omega_0)] \quad (33)$$

$$1/T_{1Z} = K[J_1(\omega_0) + 4J_2(2\omega_0)] \quad (34)$$

$$1/T_{1Q} = K[3J_1(\omega_0)] \quad (35)$$

$$1/T_{2D} = K[J_1(\omega_0) + 2J_2(2\omega_0)] \quad (36)$$

where

$$K = 2[eq/\hbar(2I-1)]^2 \quad (37)$$

These relaxation times correspond to the T_{22}, T_{66}, T_{33}, T_{77}, and T_{55} introduced by Jacobsen *et al* (5).

The spectral density functions in Eqs. 32-36 are defined as follows

$$J_0(0) = \tfrac{3}{8}\int_{-\infty}^{\infty} \overline{V_{zz}(t)\, V_{zz}(t+\tau)}\, d\tau$$

$$J_1(\omega_0) = \tfrac{1}{4}\int_{-\infty}^{\infty} \overline{[V_{zx}(t) + iV_{yz}(t)]}\,\overline{[V_{zx}(t+\tau) - iV_{zx}(t+\tau)]}\, e^{i\omega_0\tau}\, d\tau$$

$$J_2(2\omega_0)\, 1/16\int_{-\infty}^{\infty} \overline{[V_{xx}(t) + V_{yy}(t)] + 2iV_{xy}(t)]}\,\overline{[V_{xx}(t+\tau) - V_{yy}(t+\tau)] - 2iV_{xy}(t+\tau)]}\, e^{2i\omega_0\tau}\, d\tau$$

Now that the appropriate relaxation times for a spin 1 system have been introduced, the next step is to determine pulse techniques to measure each one.

It should be noted that the set of Eqs. 24-31 can easily be generalized to include the extra terms resulting from the application of an RF field and being off resonance, but their solution becomes more difficult.

B. The Free Induction Decay (FID)

When the spin system is in equilibrium and before the application of any pulses, the only coefficient of the density matrix is

$$A_4 = -2\beta_L \hbar\omega_0 = I_0 \tag{38}$$

where $\beta_L = 1/KT$. Use has been made of the high temperature approximation. After the application of an RF pulse directed along the y axis in the rotating frame of width t_ω, the nonzero coefficients are

$$A_4(0) = I_0 \cos\alpha \tag{39}$$

and

$$A_2(0) = I_0 \sin\alpha \tag{40}$$

where $\alpha = \omega_1 t_\omega$. Now the evolution of the system is governed by Eqs. 24, 26, and 27, and at a time t later

$$A_4(t) = I_0[1 - (1 - \cos\alpha)\, e^{-t/T1Z}] \tag{41}$$

$$A_2(t) = I_0 \sin\alpha\, e^{-t/T2}\{\cos\beta t + 1/(\omega_Q{}^2\omega^2 - 1)^{1/2} \sin\beta t\} \tag{42}$$

$$A_5(t) = I_0 \sin\alpha\, e^{-t/T2}\{\omega_Q/\beta \sin t\} \tag{43}$$

where

$$1/T_2 = \tfrac{1}{2}\,[1/T_{2a} + 1/T_{2b} \tag{44}$$

$$1/\gamma = \tfrac{1}{2}\,[1/T_{2b} + 1/T_{2a} \tag{45}$$

and

$$\beta^2 = \omega_Q^2 - 1/\gamma^2. \tag{46}$$

Usually $\omega_Q{}^2 >> 1/\gamma^2$ and

$$A_2 = I_0 \sin\alpha\, e^{-t/T2} \cos\omega_Q t \tag{47}$$

$$A_5 = I_0 \sin\alpha\, e^{-t/T2} \sin\omega_Q t. \tag{48}$$

In the case where $\alpha = \pi/2$, the nonzero component of the density matrix oscillates between A_2 and A_5 in the absence of an RF field.

The observed signal following a $(\pi/2)_y$ pulse will be proportional to A_2 given by Eq. 47 and an analysis of the decay of this signal can be used to obtain T_2. The Fourier transform of the FID is the frequency spectrum. Figure 1a shows a typical FID for an oriented sample and the corresponding quadrupolar split spectrum.

In powder sample, where there is a range of values for ω_Q, the decay of the FID is a result of the dephasing of the various signals from the individual crystallites in the sample as well as spin-spin relaxation. In a powder, the observed FID is proportional to

$$\int_0^1 e^{-t/T2} \cos\{\Delta_Q\{\tfrac{1}{2}(3\mu^2 - 1)\}\, T\}\, d\mu$$

where $\mu = \cos\theta$ and θ is the angle between the axis of symmetry of the electric field gradient and the direction of the applied magnetic field. Figure 1b shows a typical powder pattern FID for an unoriented sample. Notice that the first oscillation in the FID has a much larger amplitude than the succeeding ones. The Fourier transform has two well defined peaks separated by Δ_Q.

C. The Quadrupolar Echo

The nuclear signal from deuterons is generally quite weak. Experiments usually require the use of a high-Q coil to enhance the sensitivity, with the result that there is a long receiver "dead time" following an Rf pulse. This dead time may be as long as 30 μs, making it impossible to get an undistorted frequency spectrum directly from the FID. This is especially true for a powder sample where the initial part of the FID contains information about the wings of the spectrum. Because the quadrupolar splittings are associated with the time-averaged or static-quadrupolar Hamiltonian, and because $I = 1$, it is possible to circumvent the receiver dead time problem by using a two-pulse sequence which results in a quadrupolar echo (9). The pulse sequence consists of a $(\pi/2)_y$ pulse followed at a time τ later by a $(\pi/2)_x$ pulse. At another time τ later, a refocussing of the magnetization occurs. The amplitude of the echo decreases with increasing τ, however, because of irreversible losses of phase coherence due to static magnetic dipole interactions with other nuclei and fluctuating quadrupolar and dipolar interactions. In

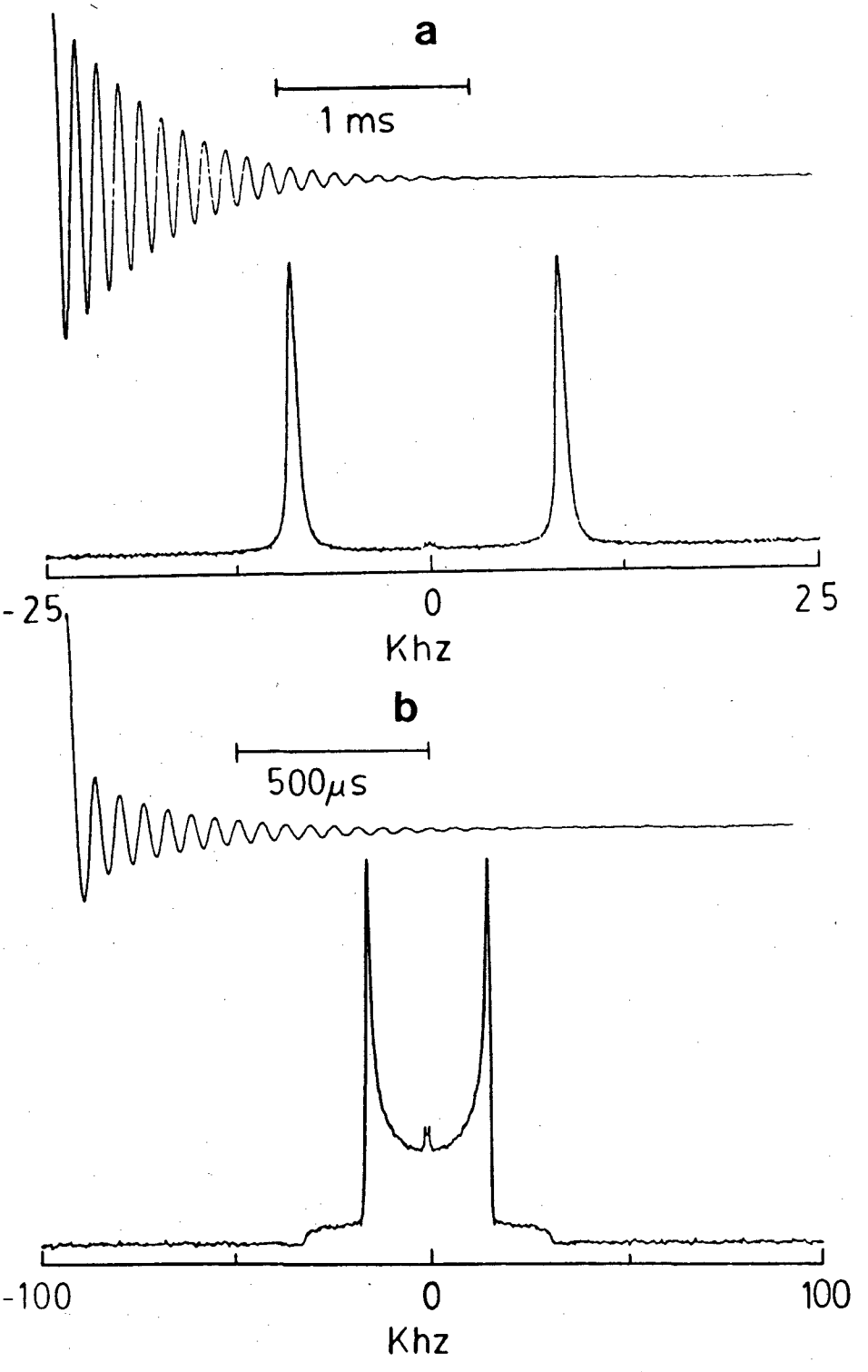

Figure 1. **(a)** The free induction decay and frequency spectrum of the deuterons in an ordered sample consisting of 30% potassium laurate-αd_2, 60% H_2O, 6% decanol, and 4% KCl at 16°C. **(b)** The free induction decay and frequency spectrum of the deuterons in a mixture of 70% rubidium stearate-αd_2 and 30% H_2O at 92°C. The free induction signals were, in fact, recorded starting at the peak of the quadrupolar echo to avoid the receiver dead time.

the theoretical outline given here, the magnetic dipolar interactions have been neglected and only relaxation due to the time-dependent quadrupolar interaction is considered. The nonzero coefficients after the first pulse are given by Eq. 47 and 48. Immediately after the $(\pi/2)_x$, the nonzero coefficients are

$$A_2(\tau) = I_0\, e^{-\tau/T_2} \cos \omega_Q \tau \qquad (49)$$

$$A_5(\tau) = I_0\, e^{-\tau/T_2} \sin \omega_Q \tau \qquad (50)$$

The density matrix develops according to Eqs. 24 and 27 and the observed signal at a time t after the second pulse is proportional to

$$A_2(t) = I_0\, e^{-(\tau+t)/T_2} \cos \omega_Q (t-\tau) \qquad (51)$$

The echo which occurs at $t = \tau$ is independent of ω_Q and is therefore very valuable in the study of powder samples. A typical quadrupolar echo signal is shown in Figure 2. The signal recorded from the center of the echo onward is a reproduction of the FID reduced in amplitude by the factor $e^{-2\tau/T_2}$. The Fourier transform of this signal gives an undistorted quadrupolar split powder pattern spectrum.

The FID shown in Figure 1b was in fact obtained using the echo technique. Generally, the first large oscillation in the FID is lost in the receiver dead time.

Figure 2 shows a sequence of echoes for a powder sample. Measurement of the amplitude of the echo as a function of τ can be used to measure T_2. If T_2 depends upon the orientation of the electric field gradient with respect to the magnetic field, an estimate of the functional dependence can be obtained from an analysis of the FT spectra for a sequence of τ values. Figure 3 shows an example where T_2 is dependent on orientation. The shape of the powder spectrum changes as the spacing between the two pulses increases. The value of T_2 taken from the decay in amplitude of the peaks in the spectra is 20% less than the value taken from near the center of the spectra.

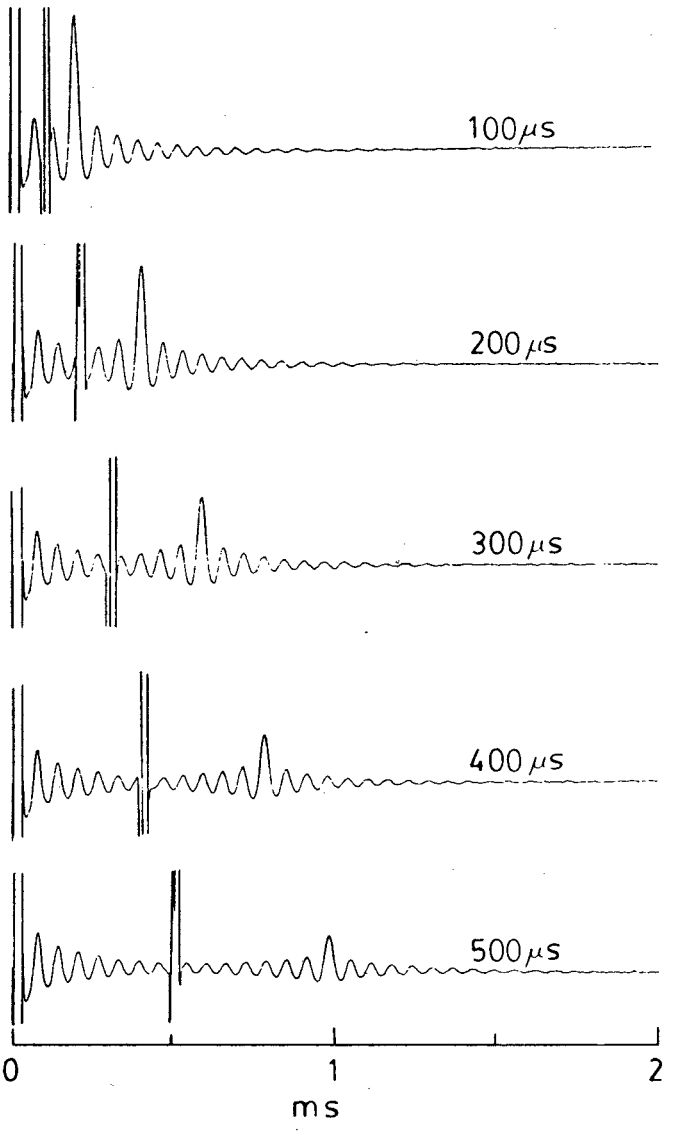

Figure 2. The quadrupolar echo in a powder sample as a function of spacing between the two pulses. The lyotropic liquid crystal sample was a mixture of 70% rubidium stearate-αd_2 and 30% H_2O at 92°C.

D. Measurement of T_{1Z}

When any RF pulse is applied to the spin system, a nonequilibrium value of the Zeeman energy results, which means that A_4 has a value different from I_0. Then, to measure T_{1Z}, $A_4(t)$ is monitored as a function of time. The most commonly used sequence of pulses is the $(\pi)_y - \tau - (\pi/2)_y$ sequence. After the first pulse

$$A_4 = -I_0 \qquad (52)$$

and at a time τ later

$$A_4(\tau) = I_0 (1 - 2e^{-\tau/T_{1Z}}) \qquad (53)$$

The amplitude of the FID following the $\pi/2$ pulse applied at time τ is proportional to $A_4(\tau)$. From measurements of FID amplitude as a function of τ, T_1 can be obtained. In a powder sample, the echo sequence is used in place of the $\pi/2$ pulse. By Fourier

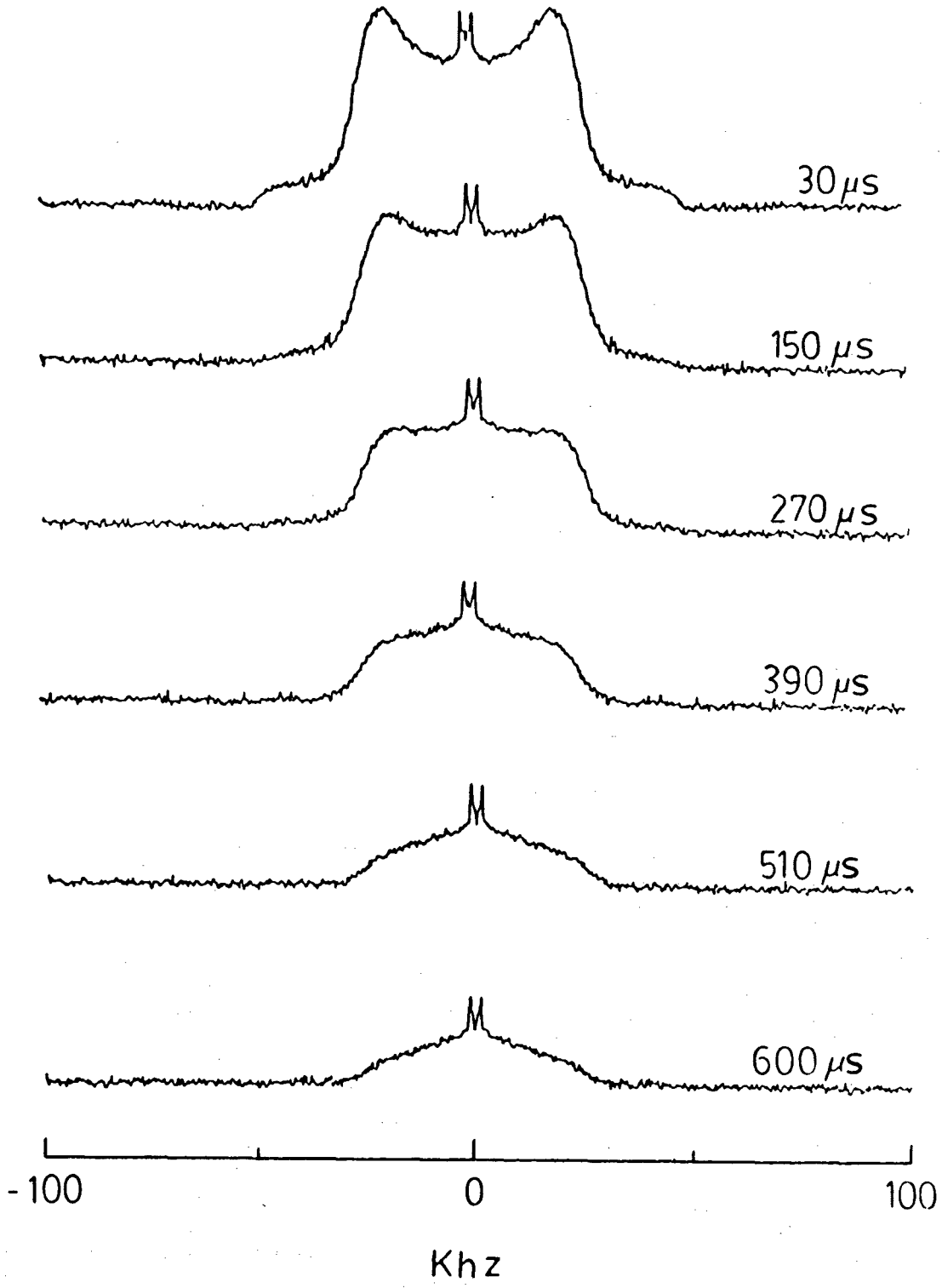

Figure 3. The Fourier transforms of a sequence of quadrupolar echoes recorded at different spacings (τ) between the two pulses. The spectra of the α deuterons in a stearate chain in a mixture of 70% rubidium stearate and 30% H_2O were recorded in the gel phase at 16°C. Notice the change in the shape of the powder pattern with increasing τ, indicating that T_2 depends on the angle betwen the electric field gradient and the magnetic field.

transforming the echo signal for each τ value, the angular dependence of T_{1z} can be obtained.

E. Creation of Quadrupolar Order

In order to measure T_{1Q}, it is necessary to create a nonzero quadrupole energy, that is, a nonzero value of the coefficient A_9. The sequence $(\pi/2)_y$ - τ_1 - $(\pi/4)_x$ results in the following nonzero coefficients immediately after the second pulse

$$A_2(\tau_1) = I_0\, e^{-\tau 1/T2} \cos \omega_Q \tau_1 \quad (54)$$

$$A_8(\tau_1) = (I_0/2)\, e^{-\tau 1/T2} \sin \omega_Q \tau_1 \quad (55)$$

$$A_9(\tau_1) = -(I_0/2)\, e^{-\tau 1/T2} \sin \omega_Q \tau_1 \quad (56)$$

With an oriented sample, it is possible to apply the second pulse such that $\cos \omega_Q \tau_1 = 0$ and $\tau_1 << T_2$. Using this sequence, it is possible to transform the original Zeeman order into a mixture of quadrupolar order and double-quantum coherence as signified by nonzero values of A_9 and A_8. In a powder, it is not possible to satisfy the condition $\omega_Q \tau = \pi/2$ for all domains in the sample. If this sequence is used, there will always be a variation in the quadrupolar order across the sample.

F. The Observation of Quadrupolar Order and Measurement of T_{1Q}

After the creation of quadrupolar order, the nonzero coefficients of the density matrix evolve according to Eqs. 24,26,27,30, and 31. The coefficient A_9 will decay with characteristic time T_{1Q}. At a time τ after the creation of the quadrupolar order, the nonzero coefficients are

$$A_2(\tau) = I_0 \cos \omega_Q \tau_1\, e^{-\tau 1/T2} \cos \omega_Q \tau \quad (57)$$

$$A_4(\tau) = I_0 (1 - e^{-\tau 1/T1Z}) \quad (58)$$

$$A_5(\tau) = I_0 \cos \omega_Q \tau_1\, e^{-\tau 1/T2} \sin \omega_Q \tau \quad (59)$$

$$A_8(\tau) = (I_0/2) \sin \omega_Q \tau_1\, e^{-\tau 1/T2D} \quad (60)$$

$$A_9(\tau) = -(I_0/2) \sin \omega_Q \tau_1\, e^{-\tau 1/T1Q} \quad (61)$$

where it has been assumed that $\tau_1 / T_2 << 1$.

Since the coefficient A_9 is not directly observable, a second $(\pi/4)_x$ pulse must be applied in order to convert A_9 into A_5. At a time t after the $(\pi/4)_x$ pulse

$$A_2(t) = I_0 e^{-\tau/T2} \cos \omega_Q \tau_1 \cos \omega_Q \tau\, e^{-t/T2} \cos \omega_Q t + (I_0/4)(e^{-\tau/T2D} + 3e^{-\tau/T1Q}) \sin \omega_Q \tau_1\, e^{-t/T2} \sin \omega_Q t \quad (62)$$

$$A_3(t) = -(I_0/\sqrt{2})(1 - e^{-\tau/T1Z})\, e^{-\tau/T2} \cos \omega_Q t \quad (63)$$

$$A_4(t) = I_0/\sqrt{2})(1 - e^{-\tau/T1Z}) \quad (64)$$

$$A_5(t) = I_0 e^{-\tau/T2} \cos \omega_Q \tau_1 \cos \omega_Q \tau\, e^{-t/T2} \sin \omega_Q t - (I_0/4)(e^{-\tau/T2D} + 3e^{-\tau/T1Q}) \sin \omega_Q \tau_1\, e^{-t/T2} \cos \omega_Q t \quad (65)$$

In an oriented sample where there is a single value of ω_Q, it is possible to make $\omega_Q \tau_1 = \pi/2$ so that

$$A_2(t) = (I_0/4)(e^{-\tau/T2D} + 3e^{-\tau/T1Q} \sin \omega_Q t \quad (66)$$

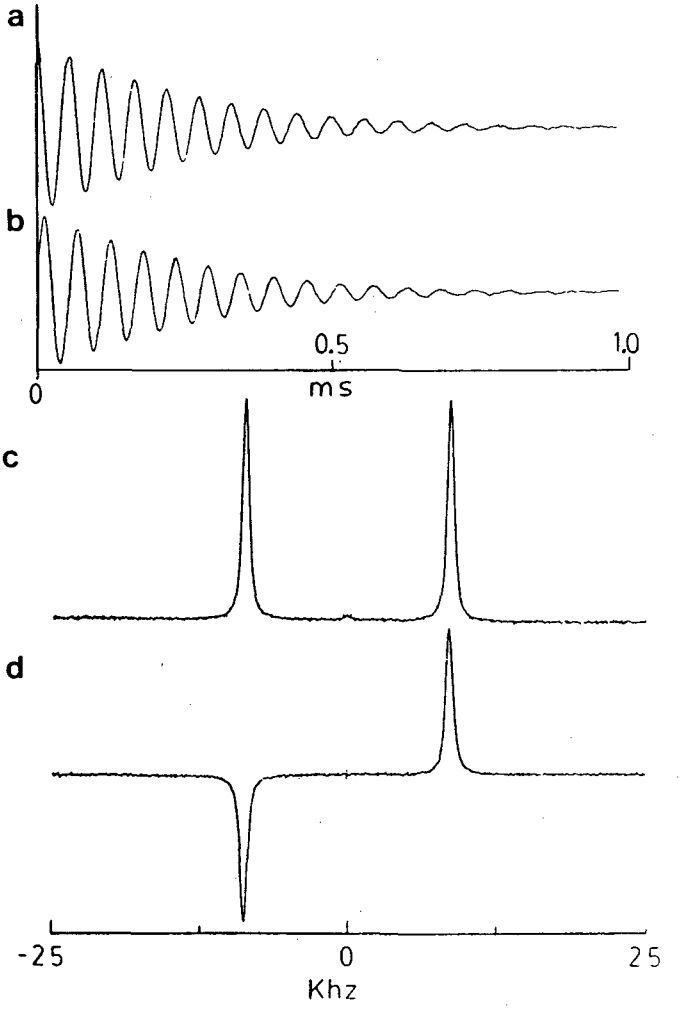

Figure 4. (a,b) The nuclear signals observed in the two detector channels following the second $(\pi/4)_x$ pulse in the Jeener - Broekaert sequence, $(\pi/2)_y$ - τ_1 - $(\pi/4)_x$ - τ - $(\pi/4)_x$. The signals are 90° out of phase. (c,d) The Fourier transforms of each signal taken separately. The Zeeman order in the spin system is proportion to the amplitudes of the signals in (a) and (c) while the quadrupolar order is proportional to the signals in (b) and (d).

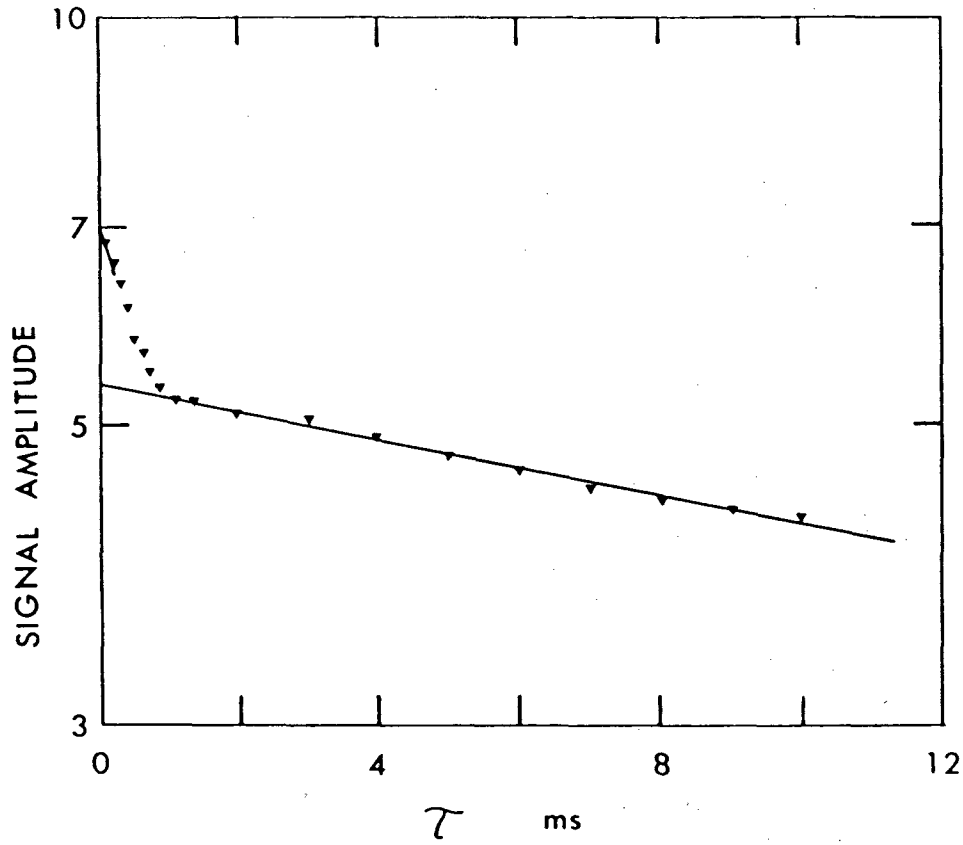

Figure 5. The decay of the signal as a function of τ for the $(\pi/2)_y$ - τ_1 - $(\pi/4)_x$ - τ - $(\pi/4)_x$ sequence. τ_1 was held constant at 22 μs. The decay follows the predicted behaviour. It is proportional to $(e^{-\tau/T_{2D}} + 3e^{-\tau/T_{1Q}})$. The ordered sample was a mixture of 30% potassium laurate-αd_2, 60% H_2O, 6% decanol, and 4% KCl at 6°C.

$$A_3(t) = -(I_0/\sqrt{2})(1 - e^{-\tau/T_{1Z}})\, e^{-t/T_2} \cos \omega_Q t \qquad (67)$$

Notice that the two signals which oscillate with frequency ω_Q are 90° out of phase. The signal in the X channel which is proportional to $A_2(t)$ is zero at $t = 0$, in contrast to the FID following the first $(\pi/2)_y$ pulse which has a maximum at $t = 0$. Figure 4 shows the signals in the two detector channels for the oriented sample as well as the Fourier transforms of these signals. Zeeman order is characterized by the usual doublet spectrum, while quadrupolar order results in an absorption signal for one peak and an emission signal for the other. By measuring the amplitudes of these two signals at a fixed time t and as a function of τ, the relaxation times T_{2D}, T_{1Q}, and T_{1Z} can be determined.

The interesting prediction of Eq. 66 is that one quarter of the signal should decay with a time constant T_{2D} and three quarters with a time constant T_{1Q}. In Figure 5, the amplitude of the signal in the X channel is shown as a function of the spacing (τ) between the two $(\pi/4)_x$ pulses. The decay is definitely the sum of two exponentials. The amplitudes of the two components are approximately in the ratio of 1 to 3 as expected. The measured values of T_{2D} and T_{1Q} at 6°C for the ordered sample were 440 μs and 43 ms, respectively.

In a multi-domain sample, Eqs. 62-65 must be considered. The first term in the expression of A_2 could complicate the measurement of T_{2D} and T_{1Q}. The spin-spin relaxation times T_2 and T_{2D} are, however, often much shorter then T_{1Q}, so that the first term in the expression for A_2 can be neglected. Observations of A_2 and A_3 in this situation can be used to obtain T_{1Q} and T_{1Z}.

Because of the dead time of the receiver, measurement of the entire FID is difficult, precluding any chance of getting an undistorted signal following the second $(\pi/4)_x$ pulse. Consequently measurements of T_{1Z} and T_{1Q} as a function of angle from the powder pattern are difficult. The problem of receiver dead time can be overcome by applying another $(\pi/2)_x$ pulse to create an echo. If the $(\pi/2)_x$ pulse is applied at time t_1, then the essential coefficients at a time t later are

$$A_2(t) = I_0 e^{-\tau/T_2} \cos \omega_Q \tau_1 \cos \omega_Q \tau e^{-(t_1 + t)/T_2}$$
$$\cos \omega_Q (t - t_1) + (I_0/4)(e^{-\tau/T_{2D}} + 3e^{-\tau/T_{1Q}}) \qquad (68)$$
$$\sin \omega_Q \tau_1 e^{-(t_1 + t)/T_2} \sin \omega_Q (t - t_1)$$

and

$$A_3(t) = (I_0/\sqrt{2})(1 - e^{-\tau/T_{1Z}})\, e^{-t/T_2} \cos \omega_Q t \qquad (69)$$

The second term in the expression for $A_2(t)$ is of principal importance. The signal arising from this term for times $t > t_1$ is identical to the signal following the second $(\pi/4)_x$ pulse, but now the effective start of the signal is at $t = t_1$ and is not lost in the receiver dead time. Figure 6 shows that changing t_1 effectively moves the beginning of the signal progressively further out from the $(\pi/4)_x$ pulse. It should be noted that the beginning of the signal ($t = t_1$) is at a zero crossing because of the form of Eq. 68. As long as T_2 and T_{2D} are relatively short compared to T_{1Q}, the terms containing $e^{-\tau/T_2}$ and $e^{-\tau/T_{2D}}$ will not interfere with the measurement of T_{1Q} which is made by varying τ and measuring the amplitude of the signal in the X channel of the receiver.

In situations where it is expected that T_{1Q} depends on the angle between the electric field gradient and the static magnetic field, it is useful to Fourier transform the signal and measure T_{1Q} for several values of ω_Q. It is possible to start digitizing the signal at $t = t_1$, then Fourier transform to obtain a frequency spectrum. The shape of the spectrum is similar to the derivative of the usual quadrupolar powder pattern. It was pointed out previously that in a powder sample it is not possible to transfer the Zeeman order entirely into quadrupolar order, hence the factor sin $\omega_Q \tau_1$ in Eq. 68. Because of the dependence on sin $\omega_Q \tau_1$, the Fourier transformed signal will have a complicated shape reflecting the fact that the conversion from Zeeman to quadrupolar order varies across the wide frequency spectrum. The conversion is maximized in the part of the line where $\omega_Q \tau_1 = \pi/2$. Figure 7 shows the change in the shape of the nuclear signal with τ_1. The Fourier transforms of these signals starting at $t = t_1$ are shown in Figure 8.

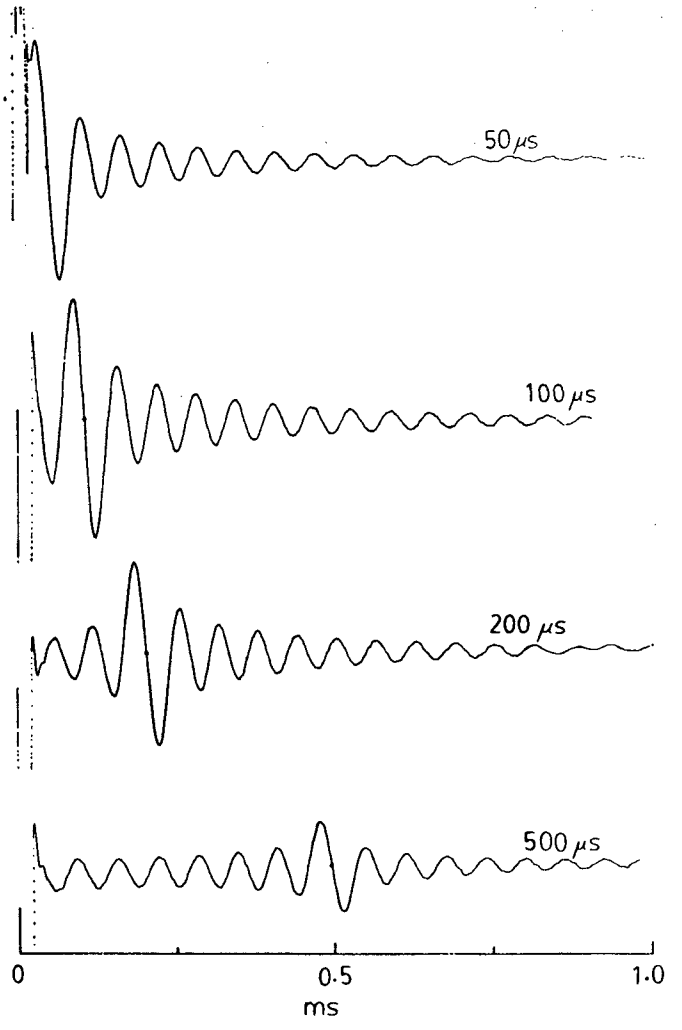

Figure 6. The effect of changing the spacing t_1 in the sequence $(\pi/2)_y$ - τ_1 - $(\pi/4)_x$ - τ - $(\pi/4)_x$ - t_1 - $(\pi/2)_x$. The effective beginning of the signal (indicated by the dot) is moved progressively further away from the final $(\pi/4)_x$ pulse as t_1 is increased. The powder sample contained 70% rubidium stearate-αd_2 and 30% H_2O held at 92°C.

The angular dependence of T_{1Q} can be obtained by collecting spectra for a variety of values of τ at a fixed τ_1. The decay of the amplitude at a number of different frequencies can be analysed to obtain the dependence of T_{1Q} on ω_Q, which in turn depends on the angle θ. In Figure 9, the Fourier transformed signals for a number of τ values are shown. An

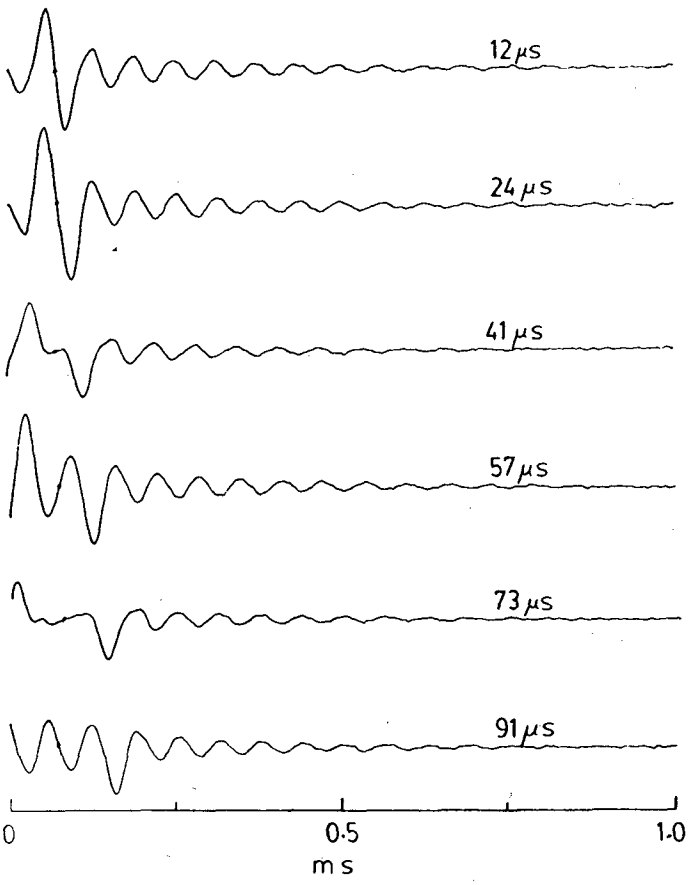

Figure 7. The effect of changing τ_1 in the pulse sequence $(\pi/2)_y$ - τ_1 - $(\pi/4)_x$ - τ - $(\pi/4)_x$ - t_1 - $(\pi/2)_x$. As τ_1 changes, the condition $\omega_Q\tau_1 = (2N + 1)(\pi/2)$ is satisfied at different parts of the powder pattern. The most efficient conversion of Zeeman into quadrupolar order then shifts to a different part of the line, causing the change in the shape of the echo. Echo signals are shown for several values of τ_1.

analysis shows that T_{1Q} varies about 20% across the frequency spectrum.

While the signal following this pulse sequence can in principle be used to obtain both T_{1Q} and T_{2D}, it would be useful to have a method of measuring T_{2D} separately since only one-fourth of the signal decays with a time constant T_{2D}. A modification of the previous sequence removes the dependence of the final signal amplitude on T_{1Q}.

G. Creation of Double-Quantum Coherence and Measurement of T_{2D}

One pulse sequence which can be used to measure T_{2D} is $(\pi/2)_y$ - τ_1 - $(\pi/4)_x(\pi/2)_y$ - τ - $(\pi/4)_x$. The nonzero coefficients of the density matrix following the first $(\pi/4)_x$ pulse are given by Eqs. 54-56.

The applicaton of a $(\pi/2)_y$ pulse immediately after the $(\pi/4)_x$ pulse eliminates the quadrupolar order, or A_9 component of the density matrix. After the $(\pi/2)_y$ pulse, the spin system evolves in the absence of any RF field according to Eqs. 26 and 30 for a time τ. At that point, the nonzero coefficients are

$$A_4(\tau) = I_0\{e^{-\tau/T2}\cos\omega_Q\tau_1 - 1)e^{-\tau/T1Z} + 1\} \quad (70)$$

and

$$A_8(\tau) = I_0 e^{-\tau_0\Sigma x}\sin\omega_Q\tau_1\, e^{-\tau/T2D}. \quad (71)$$

It is the decay of the A_8 coefficient with τ which is to be determined but, in order to monitor the decay, this coefficient must be rotated into one of the coefficients that can be directly observed. Such rotation can be brought about applying another $(\pi/4)_x$ pulse. The observed signals which appear in the two channels of the receiver are proportional to

$$A_2(\tau) = -(I_0/2)e^{-\tau\beta/T2}\sin\omega_Q\tau_1\, e^{-\tau/T2D}\sin\omega_Q t\, e^{-\tau/T2} \quad (72)$$

and

$$A_3(t) = (I_0/\sqrt{2})\{(e^{-\tau1/T2}$$
$$\cos\omega_Q\tau_1 - 1) + 1\}\cos\omega_Q t\, e^{-t/T2}. \quad (73)$$

In an oriented sample it is possible to make $\omega_Q\tau_1 = \pi/2$. Then

$$A_2(t) = -(I_0/2)\, e^{-\tau1/T2}\, e^{-\tau/T2D}\sin\omega_Q t\, e^{-t/T2} \quad (74)$$

and

$$A_3(t) = (I_0/\sqrt{2})(1 - e^{-\tau/T1Z})\cos\omega_Q t\, e^{-t/T2}. \quad (75)$$

Notice that both observed signals oscillate with angular frequency ω_Q and are 90° out of phase.

By measuring the amplitudes of these signals at an appropriate value of t as a function of τ, it is possible to obtain values for T_{2D} and T_{1Z}.

In a powder sample, a wide range of ω_Q values is present, most of the signal will be obscured by the receiver dead time because of the dephasing due to different ω_Q values. The application of another $(\pi/2)_x$ pulse a time t_1 after the second $(\pi/4)_x$ pulse produces an echo in the X channel at a time t_1 later. The echo signal is proportional to

$$A_2(t) = (I_0/2)e^{-(\tau1 + t)/T2D}\, e^{-\tau/T2D}\sin\omega_Q\tau_1$$
$$\sin\omega_Q(t - t_1) \quad (76)$$

It should be noted that this particular sequence of pulses results in a single term proportional to $e^{\tau/T2D}$ even in the case of a powder sample. A value of T_{2D} can be obtained from measurements of the echo

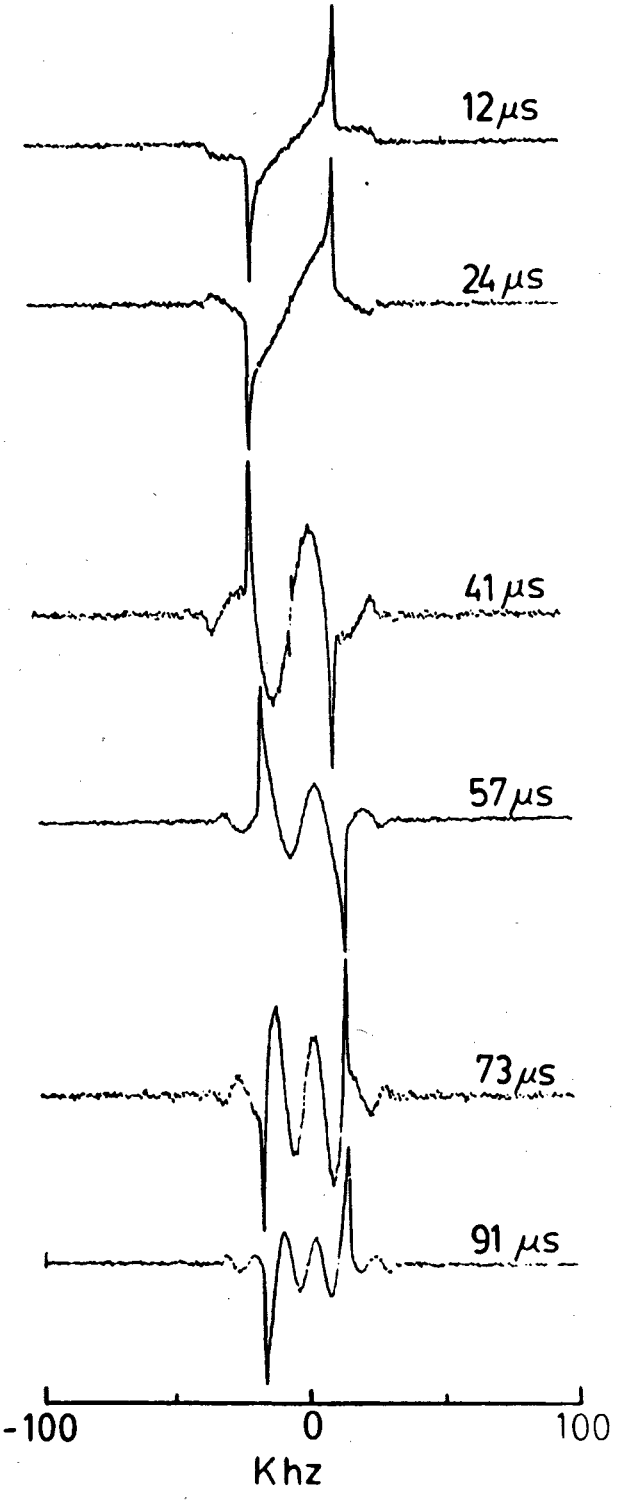

Figure 8. The Fourier transforms of the echo signals in Figure 7. The echo signal to be transformed was started at the dot indicated in the traces in Figure 7. As τ_1 increases, the effect of the factor $\sin \omega_1 \tau_1$ is very evident. The powder sample contained 70% rubidium stearate-αd_2 and 30% H_2O held at 92°C.

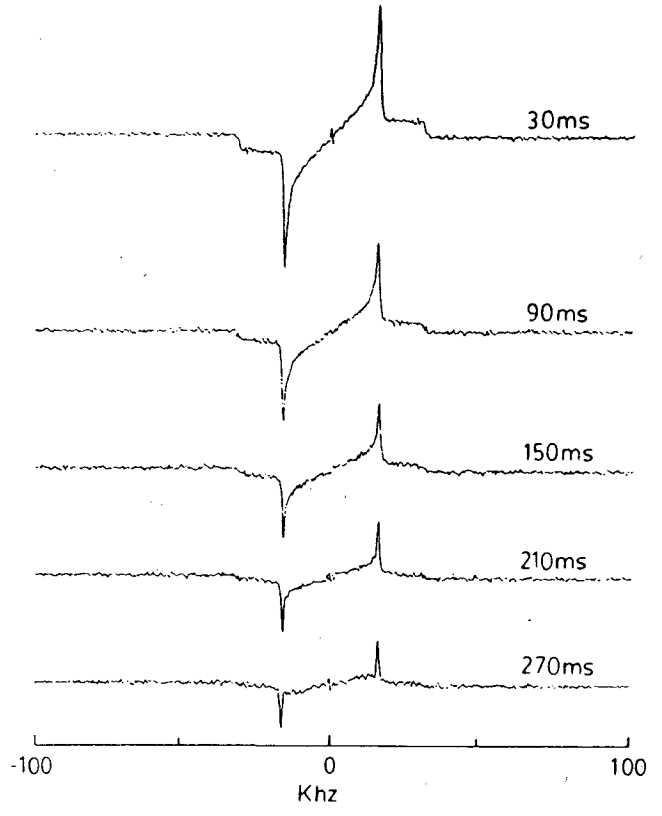

Figure 9. The decay of the quadrupolar order in a powder sample consisting of 70% rubidium stearate-αd_2 and 30% H_2O held at 92°C. The value of T_{1Q} varies about 20% across the spectrum.

amplitude as a function of τ. If T_{2D} is dependent on the angle between the electric field gradient and the magnetic field, then Fourier transforming the signal, starting at the center of the echo, and measuring T_{2D} for various values of ω_Q will give an indication of the angular dependence. The shape of the echo and the observed powder spectra obtained from Fourier transforming the echo will be similar to those observed in the measurement of T_{1Q} and shown in Figures 7 and 8.

III. CONCLUDING REMARKS

The possible relaxation times for a spin 1 system with a Zeeman-plus-quadrupolar interaction have been discussed along with the various pulse sequences needed to measure these times. The discussion started with a particularly simple Hamiltonian and the spin system was allowed to evolve in the absence of an RF field and in the on-resonance condition.

As a first step toward extending these results, it would be interesting to study the equations for the coefficients $A_j(t)$ in the presence of an RF field. Measurements made with the field on would correspond to the familiar $T_{1\rho}$ measurements presently used to advantage in spin ½ systems. It is a relatively easy task to set up the appropriate equations for the $A_j(t)$ with an RF field on (5), but their solution will be more difficult.

The next step in extending this work would be to consider other terms in the initial Hamiltonian give in Eq. 1. In particular, the dipole-dipole coupling between deuterons and currounding protons will be important in most practical applications of this work. There are two aspects to consider. The secular, or time-independent, part of this dipolar interaction will cause a dephasing of the spins as they precess, in much the same way as happens when the static magnetic field is inhomogeneous. It is probably this effect which determines the values of T_2 and T_{2D} measured for the two samples used as demonstrations of the pulse techniques in the previous section. The time-dependent part of the dipolar interaction will also be a relaxation mechanism and could contribute to the observed spin-lattice and spin-spin relaxation times in certain circumstances.

REFERENCES

[1]J. Seelig, *Quart. Rev. Biophys.* **10**, 353 (1977).
[2]H.H. Mantsch, H. Saito, and I.C.P. Smith, *Prog. NMR Spectr.* **11**, 211 (1977).
[3]J.H. Davis, K.R. Jeffrey, and M. Bloom, *J. Magn. Reson.* **29**, 191 (1978).
[4]M.F. Brown, J. Seelig, and U. Haberlen, *J. Chem. Phys.* **70**, 5045 (1979).
[5]J.P. Jacobsen, H.H. Bildsoe, and K. Schaumberg, *J. Magn. Reson.* **23**, 153 (1976).
[6]J.P. Jacobsen and K. Schaumberg, *J. Magn. Reson.* **24**, 173 (1976).
[7]R.R. Vold and R.L. Vold, *J. Chem. Phys.* **66**, 4018 (1977).
[8]A.G. Redfield, *Adv. Magn. Reson.* **1**, 1 (1965).
[9]J.H. Davis, K.R. Jeffrey, M. Bloom, M.I. Valic, and T.P. Higgs, *Chem. Phys. Lett.* **42**, 390 (1976).
[10]S.B. Ahmad and K.J. Packer, *Mol. Phys.* **37**, 47 (1979).
[11]S.B. Ahmad and K.J. Packer, *Mol. Phys.* **37**, 59 (1979).
[12]J. Jeener and P. Broekaert, *Phys. Rev.* **157**, 232 (1967).
[13]S. Vega and A. Pines, *J. Chem. Phys.* **66** 5624 (1977)
[14]R.C. Long, *J. Magn. Reson.* **12** 216 (1973).
[15]R.A. Hoffmann, *Adv. Magn. Reson.* **4**, 84 (1970).
[16]A. Wokaun and R.R. Ernst, *J. Chem. Phys.* **67**, 1752 (1977).